Commun Nonlinear Sci Numer Simulat 18 (2013) 938–945

Contents lists available at SciVerse ScienceDirect

Commun Nonlinear Sci Numer Simulat

journal homepage: www.elsevier.com/locate/cnsns

Noise and coupling induced synchronization in a network of chaotic neurons

Marzena Ciszak [a,*], Stefano Euzzor [a], Andrea Geltrude [a], F. Tito Arecchi [a,b], Riccardo Meucci [a]

[a] CNR-Istituto Nazionale di Ottica, Largo E. Fermi 6, 50125 Firenze, Italy
[b] Dipartimento di Fisica, Università di Firenze, Sesto Fiorentino (FI), Italy

ARTICLE INFO

Article history:
Received 16 May 2012
Received in revised form 30 July 2012
Accepted 27 August 2012
Available online 16 September 2012

Keywords:
Network synchronization
Electronic neurons
Common noise
Diffusive coupling

ABSTRACT

The synchronization in four forced FitzHugh–Nagumo (FHN) systems is studied, both experimentally and by numerical simulations of a model. We show that synchronization may be achieved either by coupling of systems through bidirectional diffusive interactions, by introducing a common noise to all systems or by combining both ingredients, noise and coupling together. Here we consider white and colored noises, showing that the colored noise is more efficient in synchronizing the systems respect to white noise. Moreover, a small addition of common noise allows the synchronization to occur at smaller values of the coupling strength. When the diffusive coupling in the absence of noise is considered, the system undergoes the transition to subthreshold oscillations, giving a spike suppression regime. We show that noise destroys the appearance of this dynamical regime induced by coupling.

1. Introduction

The well-known FHN model [1,2] provides arguably the simplest representation of excitable dynamics. It has been derived from the Hodgkin–Huxley model (HH) [3] describing originally the action potential propagation in the axon of the giant squid. The electrical pulses arise because the membrane of the axon is preferentially permeable to various chemical ions with the permeabilities altered by the present currents and potentials. Due to the complexity of HH, various simpler mathematical models, which still capture the key features of the full system, have been proposed, among them the FHN. FHN alone, since it is two dimensional, may exhibit only regular dynamics. Chaotic spiking regime can be created in FHN by introducing a third slow refractory variable [4,5]. Chaotic behavior can be also observed in the periodically driven FHN [6]. Such chaotic mixed-mode oscillations (chaotic small amplitude oscillations interrupted by large spikes) were first discovered in the Belousov–Zhabotinsky reaction [7] and, since then, have been frequently observed in experiments and models of chemical and biological rhythms [8] as well as in optical systems [9]. Moreover, FHN has been widely used to investigate the effects of noise. Stochastic resonance effects, that optimize information transmission have been investigated in Ref. [10] and noise enhanced stability phenomena due to the correlation time of the noise have been investigated in Ref. [11].

A clear way to distinguish excitable pulses triggered deterministically (i.e. by a chaotic background) from those triggered stochastically (i.e. by externally added noise) is the probability distribution of the inter-spike intervals (ISI). In the presence of noise, excitable systems respond by random spiking on a noisy background, with a mean firing rate that increases with the noise amplitude and with an exponentially vanishing ISI distribution cutoff at the refractory time [12]. In the chaotic spiking

* Corresponding author.
E-mail address: marzena.ciszak@ino.it (M. Ciszak).

1007-5704/$ - see front matter © 2012 Elsevier B.V. All rights reserved.
http://dx.doi.org/10.1016/j.cnsns.2012.08.038

regime, instead, there are no external forces, the aperiodic background triggers excitable spikes in an erratic but completely deterministic sequence [13].

The synchronization of coupled systems, that describe the features of neural dynamics, has been a subject of intensive studies and regarded various topologies, including global all-to-all [14] or local [15,16] coupling configurations. Recently, it has been shown, that it is possible to induce synchronization in two FHN by a common noise [17] and that the correlated noise gives stronger synchronization at lower noise amplitude with respect to that of uncorrelated noise. In this paper we extend the previous work and study experimentally and numerically the relation between the two different ways of inducing synchronization, namely, by common noise and by direct coupling. Here we consider a network composed of $N = 4$ oscillators. We show that, as clearly expected, the common noise leads to synchronization, but what is more interesting, the addition of common noise allows the synchronization to occur at smaller values of the coupling strength, thus enhancing the synchronization induced by coupling. We show that the colored noise is more efficient in enhancing the synchronization between the systems than the white noise. When the diffusive coupling in the absence of noise is considered, we observe that the system undergoes dynamical changes consisting of the spike suppression phenomenon, leading the system to subthreshold oscillations. We show that noise destroys the appearance of this dynamical regime. In addition to experiment, we consider a simple model equations describing FHN with periodic forcing and reproduce all the qualitative characteristics of the synchronization process observed in the experiment.

2. Experimental setup and the model

A network of four FHN has been realized on printed circuit, planned by using OrCad. The electronic network is implemented by means of a nearest neighbor closed loop coupling scheme, as shown in Fig. 1. The scheme for the electronic circuit reproducing each FHN is shown in Fig. 2, meanwhile that for the coupling implementation is shown in Fig. 3. The equations describing each FHN circuit, with a small amount of feedback signal V_f added, are the following:

$$\begin{aligned}\dot{V}_{xi} &= V_{xi} - V_{yi} - \frac{R_{5i}}{R_{1i}}V_{xi}^3 + V_d + I + \alpha\Delta V_{xi}\\ \dot{V}_{yi} &= V_{xi} - \frac{R_{2i}}{R_{1i}}V_{yi} + \frac{R_{3i}}{R_{1i}}V_{bi}\end{aligned} \tag{1}$$

where $i = 1,\ldots,4$ indicates the nodes in the network, V_d is the driving signal, I is the common (white or colored) noise signal, V_{bi} is a bias voltage and $\alpha = R_{fi}/R_{1i}$ is the coupling strength. The coupling term ΔV_{xi} is defined as:

$$\Delta V_{xi} = V_{x(i+1)} + V_{x(i-1)} - 2V_{xi} \tag{2}$$

with periodic boundary conditions. The coupling strength $\alpha = R_e/R$ is determined by a suitable value of a variable resistor. We used a random noise generator (Allison Labs, model 650) which exploits a pair of Zener diodes for white noise generation and suitable filters for colored noise outputs.

On the other side, the model equations for the driven FHN are the following:

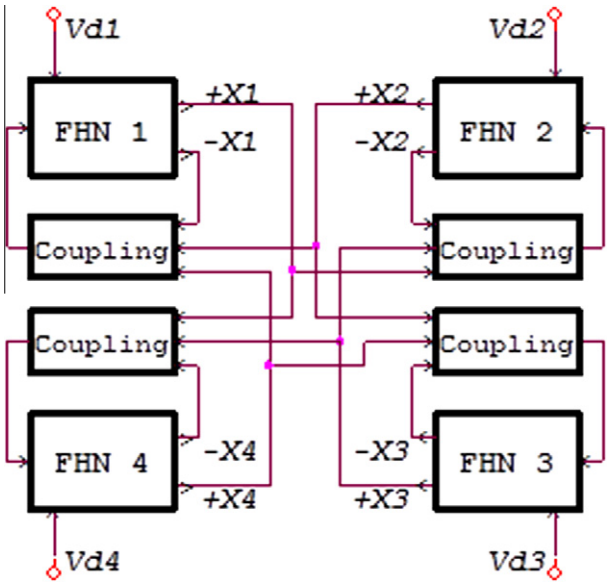

Fig. 1. Scheme for the network of four FHN. The coupling is bidirectional and the topological structure represents a ring.

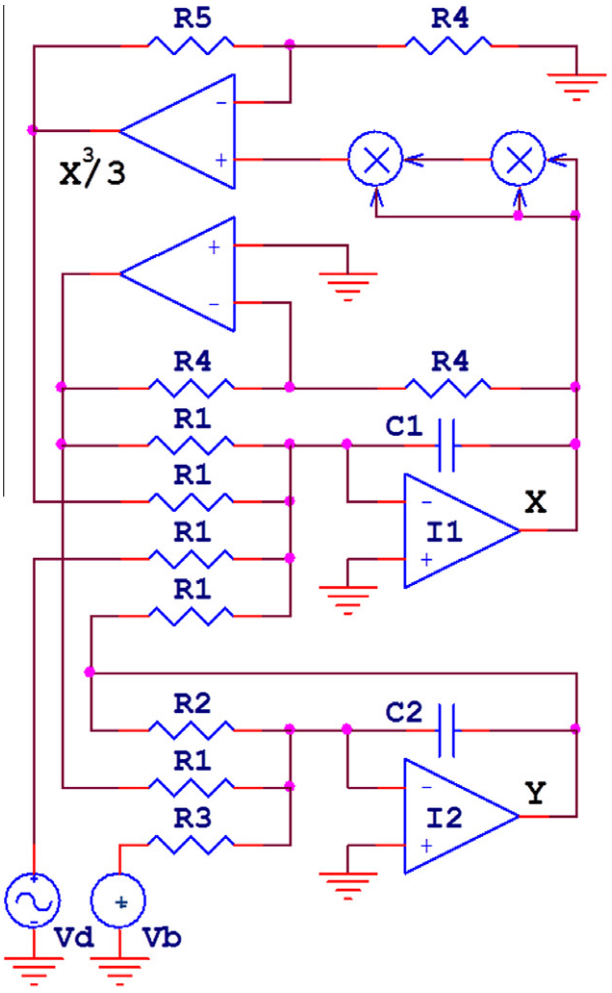

Fig. 2. Scheme of the electronic circuit implementing each driven FHN, with letters denoting I_k integrators, R_k resistors, C_k capacitors, X multipliers, V_d sinusoidal forcing signal and V_b fixed bias voltage.

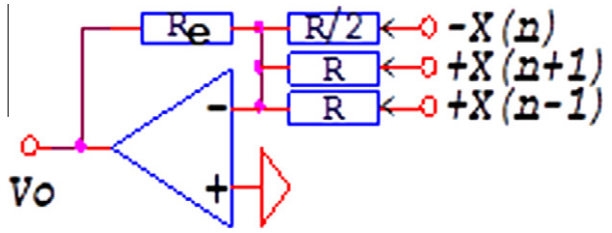

Fig. 3. Scheme for the electronic coupling. R_e e R denote resistors that control the coupling strength between the nodes.

$$\begin{aligned}\dot{x}_i &= x_i - y_i - x_i^3/3 + V_d + I + \alpha\Delta x_i \\ \dot{y}_i &= \gamma(x_i - a y_i + b)\end{aligned} \tag{3}$$

where $x_i(t)$ is the voltage variable, $y_i(t)$ is the recovery variable and $V_d = A\sin(2\pi\nu t)$ is an external driving term with amplitude A and frequency $\nu = 1/T$. We consider fixed parameters $\gamma = 0.08$, $a = 0.8$ and $b = 0.7$. Eq. (3) is transformed to the three-variable set of equations by introducing a new variable $z_i = 2\pi\nu t = \omega t$, as follows:

$$\begin{aligned}\dot{x}_i &= x_i - y_i - x_i^3/3 + A\sin z_i + I + \alpha\Delta x_i \\ \dot{y}_i &= \gamma(x_i - a y_i + b) \\ \dot{z}_i &= \omega\end{aligned} \tag{4}$$

The coupling term Δx_i is defined as:

$$\Delta x_i = x_{i-1} + x_{i+1} - 2x_i \tag{5}$$

for $i = 1, \ldots, 4$ and periodic boundary conditions. We consider the external common forcing I to be white $I = \xi(t)$ or colored $I = \epsilon(t)$ noise. White noise ξ is a Gaussian random process of zero mean and delta-correlated in time: $\langle \xi(t)\xi(t')\rangle = 2D\delta(t-t') = \sigma^2\delta(t-t'), D$ being the noise intensity and σ its standard deviation. The generation of the colored noise (Ornstein–Uhlenbeck process) ϵ is obtained by solving the following equation:

$$\dot{\epsilon} = -\eta\epsilon(t) + \eta\xi(t) \tag{6}$$

where η is a constant parameter and ξ is a white noise defined above.

3. Characterization of the single driven FHN

Modulation of parameter A starting from the zero value, at the fixed value of the frequency ω, induces the period-doubling route to chaos with the sharp windows where chaotic spiking emerges, as shown in the bifurcation diagrams of Fig. 4(a) and (b) for experimental circuit and model equations, respectively. When modulating the frequency ω of the external driving (see Fig. 4(c) and (d)), setting fixed value of the amplitude A, the system undergoes also in this case a period doubling, but with a clear mixed-mode oscillations (MMO) windows. For the selected value of parameter A, one can identify the following MMO orbits: $L^S = 1^1,\ 1^2,\ 1^4,\ 1^6$, where L stands for large amplitude spike and S for small amplitude sub-threshold oscillation. Similar cascade of MMOs has been observed in the light emitting diodes with optoelectronic feedback (see Ref. [9]). The period doubling region tends to expand in the frequency domain as the amplitude A of the external driving increases. In further study we choose fixed values of A and ω, such to obtain a chaotic spiking regime. Moreover, we introduce slight parameter mismatches between all systems in the experimental as well as in theoretical networks.

4. Evolution of generation times affected by coupling and noise

To describe quantitatively the transition to synchronization we characterize the degree of order in the system by means of entropy S is defined as:

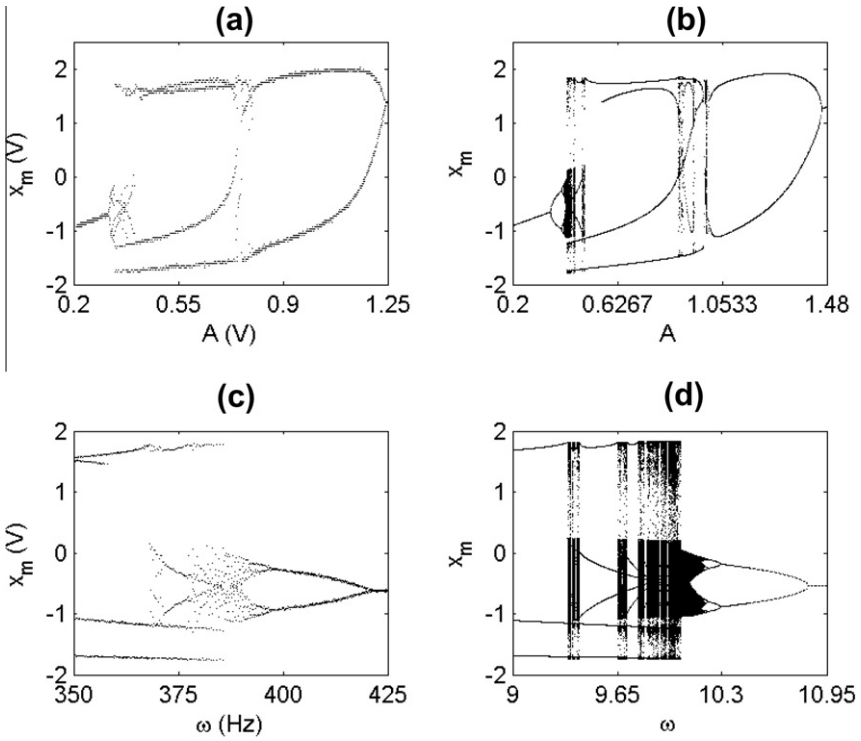

Fig. 4. Bifurcation diagrams for a single driven FHN as different control parameters vary: (a) and (b) amplitude A of the driving signal, (c) and (d) frequency of the driving signal. Diagrams in (a) and (c) are obtained experimentally and (b) and (d) numerically.

$$S = -\sum_{T_g} \rho(T_g) \ln \rho(T_g) \tag{7}$$

where $\rho(T_g)$ is the discrete probability distribution (histogram) of a continuous variable T_g. We define the generation time T_g as the time difference between spike occurrences at neighboring sites. S is calculated from the distribution of the generation times T_g in the time series, far beyond the initial transient. When the coupling and noise are absent, this distribution is flat (see Fig. 5(a) and (d), for the experiment and the model, respectively), i.e., the information on one site gives no information on the other ones. Increasing the coupling in the absence of noise, we observe the birth of peaks for fixed time differences, due to the time correlation between spikes at adjacent sites (see Fig. 5(b) and (e), for the experiment and the model, respectively).

Similar phenomenology is observed when considering common noise in the systems at zero coupling (see Fig. 5(c) and (f), for the experiment and the model, respectively). This means that common noise in the system can induce synchronization of the whole network in a similar way as the diffusive coupling. There is however a crucial difference between coupling by common noise and diffusive direct interaction, which will be discussed in more details in the next section.

In Fig. 6 we plot the magnitudes of entropy S for different values of coupling strength α and various noise amplitudes. The entropy S in Fig. 6(a) and (b) (for white and colored noises) is calculated from the experimental data, meanwhile in Fig. 6(c) and (d) (for white and colored noises) it is calculated from the numerical data. We acquired experimental data for six different values of coupling until $\alpha = 0.1$, and for seven values of noise (until $\sigma = 1\ V_{RMS}$), both for white and colored ones. Initially, when the oscillators are uncoupled and noise is not injected, all FHNs are unsynchronized, as can be seen in the raster plots in Fig. 7(a) and (c), for the experiment and the model, respectively. In this condition the entropy value for the entire system is high. Increasing noise and coupling strength, the network reaches synchronization (see raster plots in Fig. 7(b) and (d) for the experiment and the model, respectively). Both, experimental and numerical results, obtained for different levels of noise and for different values of coupling strengths, show that colored noise leads to synchronization using a smaller noise amplitude respect to that of white noise. It can be clearly seen when comparing the values of entropy reported in Fig. 6(a) and (c) (for white noise) with those in Fig. 6(b) and (d) (for colored noise).

5. Effects of noise on dynamical states of the network

In the absence of noise or when it is weak, we observe different dynamical behavior at the single node level. In a small range of coupling parameter, before the synchronized state arise, the coupling suppresses spiking dynamics giving rise to the

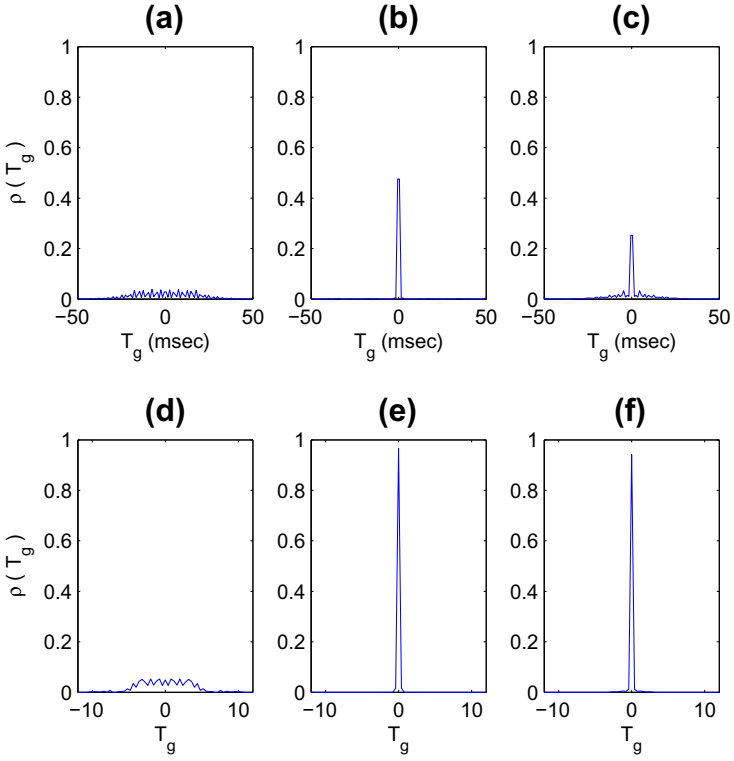

Fig. 5. Distribution of the generation times T_g in the case of white noise for the experiment: (a) $\alpha = 0$ and $\sigma = 0$, (b) $\alpha = 0.1$ and $\sigma = 0$, (c) $\alpha = 0$ and $\sigma = 1$ and for the model: (d) $\alpha = 0$ and $\sigma = 0$, (e) $\alpha = 0.1$ and $\sigma = 0$, (f) $\alpha = 0$ and $\sigma = 1(V_{RMS})$.

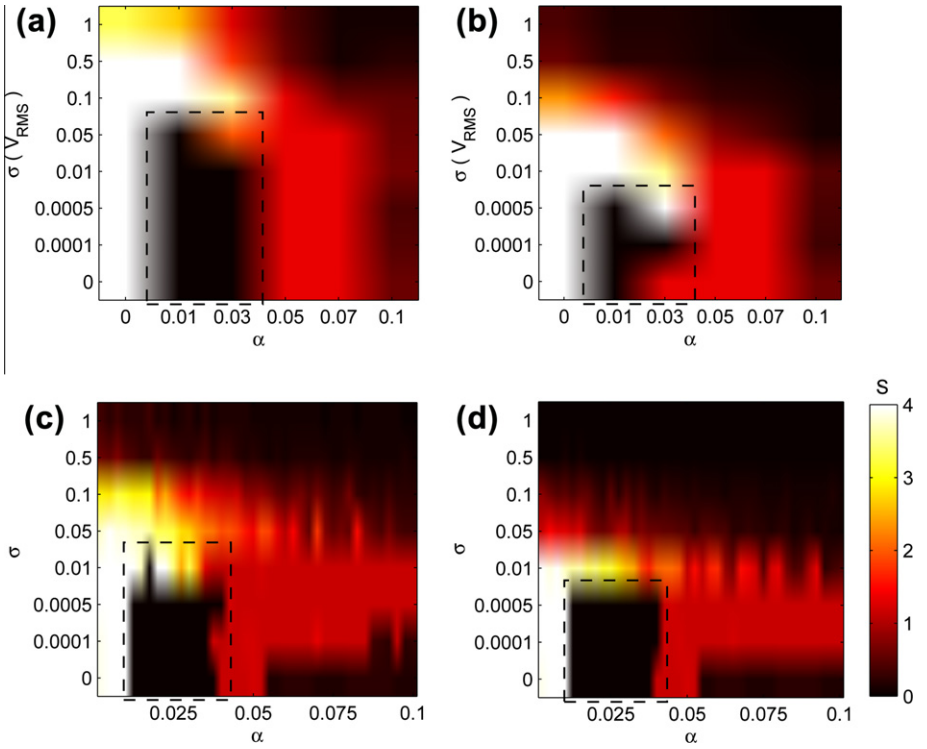

Fig. 6. Entropy S in the parameter space of α and σ calculated from the experiment for the case of white (a) and (b) colored noise, and from the model for the case of white (c) and (d) coloued noise. High values of S (light colors) correspond to uncorrelated states, meanwhile low values of S (dark colors) to correlated states. (For interpretation of the references to colour in this figure legend, the reader is referred to the web version of this article.)

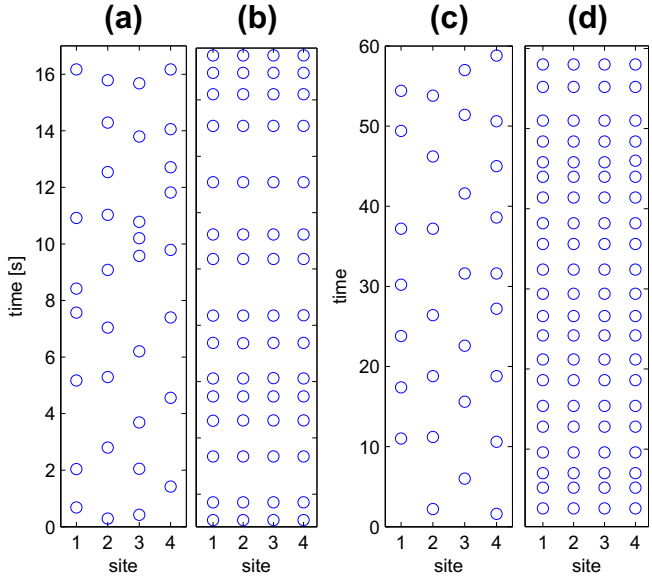

Fig. 7. Raster plot showing the spatiotemporal occurrences of spikes measured experimentally for (a) $\alpha = 0$ and $\sigma = 0$ in the absence of noise and coupling, (b) $\alpha = 0.1$ and $\sigma = 1V_{RMS}$ in the presence of coupling and white noise signal, as well as numerically for (c) $\alpha = 0$ and $\sigma = 0$ in the absence of noise and coupling, (d) $\alpha = 0.1$ and $\sigma = 1$ in the presence of coupling and white noise signal.

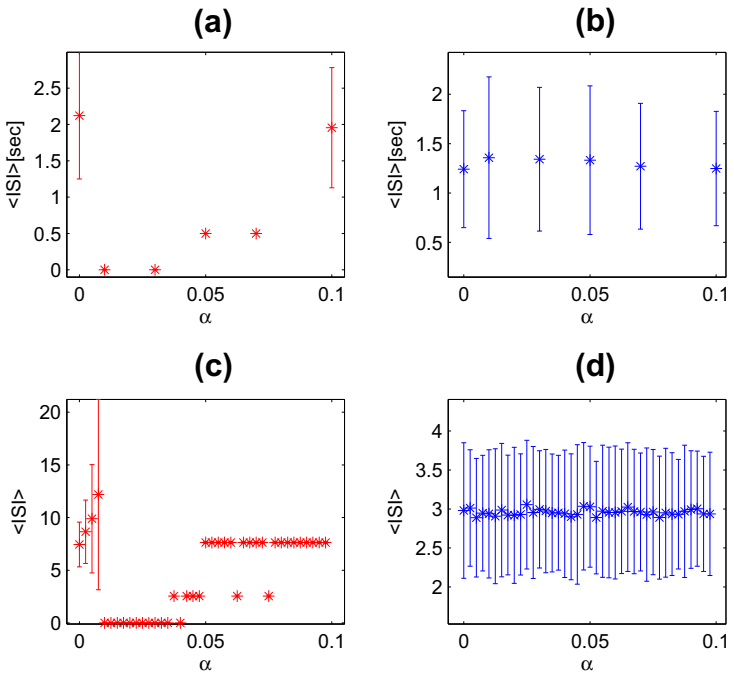

Fig. 8. Mean ISIs and their standard deviation as coupling strength α is varied calculated from the experiment: (a) the absence of noise ($\sigma = 0$) and (b) in the presence of white noise ($\sigma = 1$), as well as from the model: (c) the absence of noise ($\sigma = 0$) and (d) in the presence of white noise ($\sigma = 1$).

subthreshold oscillations. The regions (in the parameter space) where it occurs are marked by dashed-line boxes in Fig. 6. In this figure the entropy S is nonmonotonic due to a coupling effect. At zero coupling the entropy decrease is monotonic as the amplitude of noise increases. However, as the coupling is introduced to the systems and is varied, the dynamical changes in the systems emerge at a critical coupling strength. The dynamics suddenly reduces to subthreshold oscillations. As the coupling is increased further, the large amplitude spikes re-appear again, and the transition to synchronization is slowly reached. Thus, the nonmonotonicity is caused mostly by dynamical changes in the system induced solely by the coupling term.

In Fig. 8 we report the mean ISI and their standard deviations calculated from the time series of the single system in the network in the absence and the presence of white noise. In the former case, we notice that indeed in a certain range of the coupling parameter, the mean ISI goes to zero, indicating the suppression of spiking. The transition from spiking regime to spike suppression is smooth, and consist on the consequent increase of the chaotic spiking mean period, as the coupling is increased, until it reaches infinity (see the large error bars in Fig. 8(c)). On the other hand, when the common noise is present, strong enough to induce synchronization in the absence of coupling, the spike suppression zone is destroyed leading to constant mean ISI over all coupling strength. This characteristic points out the difference between the both types of synchronization generators. The phenomenon described above may be explained in terms of excitability of subthreshold oscillations [18]. At noise amplitude that is above a critical threshold, the excitable small-amplitude oscillations respond to the external perturbations with spikes that fire randomly, loosing the chaotic properties.

On one side, the introduction of common noise destructs the regimes of subthreshold oscillations. On the other side, at higher amplitudes of noise, it is able to induce spikes that synchronize. We still expect to observe the destruction of the subthreshold oscillation regime (the spikes elicited by noise since the systems remain excitable) when driving the systems with uncommon noises. However, at higher amplitudes of uncommon noises the synchronization induced by coupling should be weakened, and in the absence of coupling systems will remained highly uncorrelated.

We have calculated the entropy also for cases with $N = 10$ and $N = 40$ and we noticed that the coupling strength needed to obtain synchronization increases. Moreover, the regimes of spike suppression during the transition to synchronization become wider, suggesting the stronger effect of the system size on the nodes dynamics.

6. Conclusions

We have shown, both, experimentally and through the numerical simulations that the synchronization in a network of four forced FHN can be achieved either by coupling of systems by bidirectional diffusive interactions, by a common noise or by combining both of them. We have considered two types of noise, namely, white and colored one, and demonstrated that the colored noise is more efficient in synchronizing the systems. Moreover, the small addition of common noise allows

the synchronization to occur at smaller values of the coupling strength. During the transition to synchronization we have observed that coupling alone changes the dynamical behavior of the systems. These dynamical changes consist of suppression of spiking, leading the system to subthreshold small-amplitude oscillations. We have shown that noise destroys the appearance of this dynamical regime and explained why it happens. Precisely, it is related to the excitability of the small-amplitude oscillations, that in the presence of noise triggered erratic spikes giving rise to a revival of spiking regime.

Acknowledgments

Work partly supported by Ente Cassa di Risparmio di Firenze. MC acknowledges MC-ERG (within 7th EC Programme) and C. Ciamberlini (CNR-INO Firenze) for technical support in Centro Calcolo.

References

[1] FitzHugh R. Impulses and physiological states in theoretical models of nerve membrane. Biophys J 1961;1:445–66.
[2] Nagumo JS, Arimoto S, Yoshizawa S. An active pulse transmission line simulating nerve axon. Proc IRE 1962;50:2061–70.
[3] Hodgkin AL, Huxley AF. A quantitative description of membrane current and its application to conduction and excitation in nerve. J Physiol (London) 1952;117:500–44.
[4] Doi S, Kumagai S. Generation of very slow neuronal rhythms and chaos near the hopf bifurcation in single neuron models. J Comput Neurosci 2005;19:325–56.
[5] Marino F, Marin F, Balle S, Piro O. Chaotically spiking canards in an excitable system with 2D inertial fast manifolds. Phys Rev Lett 2007;98:074104(1)–4(4).
[6] Pankratova EV, Polovinkin AV, Spagnolo B. Suppression of noise in FitzHugh–Nagumo model driven by a strong periodic signal. Phys Lett A 2005;344:43–50.
[7] Petrov V, Scott SK, Showalter K. Mixed-mode oscillations in chemical systems. J Chem Phys 1992;97:6191–8.
[8] Iglesias C, Meunier C, Manuel M, Timofeeva Y, Delestrée N, Zytnicki D. Mixed mode oscillations in mouse spinal motoneurons arise from a low excitability state. J Neurosci 2011;31(15):5829–40.
[9] Marino F, Ciszak M, Abdalah SF, Al-Naimee K, Meucci R, Arecchi FT. Mixed mode oscillations via canard explosions in light-emitting diodes with optoelectronic feedback. Phys Rev E 2011;84:047201(1)–1(5).
[10] Stocks NG, Mannella R. Generic noise-enhanced coding in neuronal arrays. Phys Rev E 2001;64. 030902(R)(1)–030902(R)(4).
[11] Valenti D, Augello G, Spagnolo B. Dynamics of a FitzHugh–Nagumo system subjected to autocorrelated noise. Eur Phys J B 2008;65(3):443–51.
[12] Eguia MC, Mindlin GB, Giudici M. Low-frequency fluctuations in semiconductor lasers with optical feedback are induced with noise. Phys Rev E 1998;58:2636–9.
[13] Al-Naimee K, Marino F, Ciszak M, Meucci R, Arecchi FT. Chaotic spiking and incomplete homoclinic scenarios in semiconductor lasers with optoelectronic feedback. New J Phys 2009;11:073022(1)–073022(11).
[14] Arenas A, Díaz-Guilera A, Kurths J, Morenob Y, Zhoug C. Synchronization in complex networks. Phys Rep 2008;469:93–153.
[15] La Rosa M, Rabinovich MI, Huerta R, Abarbanel HDI, Fortuna L. Slow regularization through chaotic oscillation transfer in an unidirectional chain of Hindmarsh-Rose models. Phys Lett 2000;266:88–93.
[16] Ciszak M, Montina A, Arecchi FT. Sharp versus smooth synchronization transition of locally coupled oscillators. Phys Rev E 2008;78:016202(1)–2(4).
[17] Zambrano S, Mariño IP, Seoane JM, Sanjuán MAF, Euzzor S, Geltrude A, et al. Synchronization of uncoupled excitable systems induced by white and coloured noise. New J Phys 2010;12:053040(1)–053040(16).
[18] Al-Naimee K, Marino F, Ciszak M, Abdalah SF, Meucci R, Arecchi FT. Excitability of periodic and chaotic attractors in semiconductor lasers with optoelectronic feedback. Eur Phys J D 2010;58:187–9.